Development of Polyaniline-Polydimethylsiloxane Adduct Nanoparticle Dispersed Butylated Melamine Formaldehyde Cured Soy Alkyd

Sharif Ahmad, Ufana Riaz, Mohd Kashif, Mohd Shoeb Khan

Materials Research Laboratory, Department of Chemistry, Jamia Millia Islamia University, New Delhi-110025, India

Received 11 April 2011; accepted 23 May 2011
DOI 10.1002/app.34942
Published online 4 October 2011 in Wiley Online Library (wileyonlinelibrary.com).

ABSTRACT: Inherently conducting polymers (ICP) have attracted the attention of researchers because of their low cost and environmental stability. However, for commercial applications the poor processibility and solubility of ICPs have inhibited their widespread use. To avoid these disadvantages adducts, blends, and composites of conducting polymers have been developed. With a view to enhance the processibility of polyaniline (PANI), this work reports the synthesis of nano PANI polydihydroxydimethylsiloxane (PDMS) adduct and the formulation of its nanocomposite via the dispersion of this nano adduct in butylated melamine formaldehyde (BMF) cured soy alkyd (SA) in different weight loadings (0.25 wt %, 0.5 wt %, 1 wt %). The formation of PANI-PDMS adduct and its dispersion in butylated melamine formaldehyde (BMF) cured soy alkyd (SA) was confirmed by FTIR, UV-visible, ^{1}H-NMR whereas the morphological characterization was done using TEM and X-ray diffraction analyses. The presence of PANI-PDMS in SA-BMF resin was found to significantly enhance the physicochemical, physicomechanical, and thermal properties which could be utilized in the development of corrosion protective paints and coatings. © 2011 Wiley Periodicals, Inc. J Appl Polym Sci 124: 365–372, 2012

Key words: nanocomposites; morphology; conducting polymers; soy alkyd

INTRODUCTION

Conducting polymers like polyaniline (PANI), polyacetylene (PA), polypyrrole (Ppy), polythiophene (PTh), and poly(phenylenevinylene) (PPV) are regarded as new generation polymers as they show immense potential in various technological applications such as sensors, batteries, electrochemical displays, catalyst, antistatic coatings, anticorrosive coatings, electromagnetic shielding, functional membranes, controlled release of ionic drugs etc.[1–6] Among them, PANI has been extensively studied because of its relatively good conductivity and ease of preparation. However, the brittle nature and poor processibility of PANI limits its commercialization.[7]

One of the most common techniques adopted to improve the processibility of PANI is by the introduction of alkyl or alkoxy chain into the meta or ortho position of the aniline ring thereby enhancing its solubility in different organic solvents. It has been reported that the synthesis of both ring and *N*-sulfonated PANI has shown to improve the solubility of the former in water.[8–11] PANI and its modified forms exist in different oxidation states which find immense potential for application as corrosion inhibitors.[12–18] An alternative technique is the incorporation of PANI into organic polymers by chemical polymerization, grafting, mechanical mixing, *in situ* polymerization, or copolymerization.[19–20]

Organosilanes are one of the important alternatives to organic polymers used as binders and adhesion promoters. Dihyhroxydimethylsiloxane (DDMS) acts as a binder through adhesion between polymer and metallic/nonmetallic surfaces.[21,22] Alkyd resins are a complex network oil-based polyesters widely used in the paints and coatings industry.[23] The rapidity of the drying process as well as the hardness of the final coating material depends upon the amount and nature of fatty acid chains incorporated into the alkyd resin and their degree of unsaturation.[24] The technology of siloxane modified alkyd for high temperature service coatings has been fairly well established.[25] Curing of hydroxyl group containing long-oil air-drying alkyds with reactive silicone intermediates has been used to improve the durability, flexibility, gloss retention, and increased thermal resistance of the coating.[26,27] Silicone-cured hydroxylated polyesters have high heat resistance and outstanding exterior durability.[28,29]

Scant work has been reported on the synthesis of PANI-PDMS nanocomposites.[30] In this study, PANI-PDMS nano adduct was prepared via *in situ*-polymerization of aniline in presence of PDMS. The

Correspondence to: S. Ahmad (sharifahmad_jmi@yahoo.co.in).

Contract grant sponsor: Naval Research Board (NRB); contract grant number: DNRD/05/4003/155.

dispersion of PANI-PDMS adduct was carried out using different loadings (0.25 wt %, 0.5 wt %, and 1.0 wt %) of the former in butylated melamine formaldehyde (BMF) cured soy alkyd (SA). The resulting nanocomposites were characterized by spectral, morphological, thermal, physicochemical, and physicomechanical studies. Remarkable improvement in the physicochemical and physicomechanical properties of the nanocomposite was noticed as compared with other reported PANI/alkyd nanocomposites.[23] These nanocomposites may find promising application in the field of corrosion protective paints and coatings.

EXPERIMENTAL

Materials

Soy alkyd (SA) was procured from Shankar dyes and Chemicals (Delhi, India). Aniline (C_6H_7N) (Merck-Germany) was distilled twice under reduced pressure and stored in a refrigerator prior to its use. Ethyl Methyl Ketone (EMK) (ς-Aldrich, USA), dihydroxy dimethyl silane (DDMS) (Aldrich, USA), ammonium persulphate (Sd Fine Chemicals, Mumbai, India) zinc chloride ($ZnCl_2$) (ς-Aldrich, USA) were used as received.

Synthesis of BMF-cured SA

The BMF cured SA resin was prepared by mixing SA and BMF in ethyl methyl ketone (EMK) under vigorous stirring at 80°C. The curing of SA with BMF was carried out using different weight percent loadings of BMF as curing agent, i.e., 40, 50, and 60 wt %. It was observed that the coatings at 40 wt % BMF failed to dry at ambient temperature due to incomplete curing of SA with BMF, while the coatings with composition beyond 60 wt % BMF were found to be brittle, which could be attributed to excessive crosslinking between SA and BMF. Hence, the resin with optimum composition of SA-BMF (i.e., SA-BMF-60) was chosen for the dispersion of PANI-PDMS adduct as the coatings were found to cure at ambient temperature and form well-adherent coatings on mild steel (MS).

^{1}H-NMR spectra of SA/BMF ($CDCl_3$) δ (ppm): 7.71 ($C_6\mathbf{H}_6$), δ (ppm): 4.35 (—C$\mathbf{H}_2$—OCOR),3.79 (—C$\mathbf{H}$ —), 3.8 (C$\mathbf{H}_2$—), 4.5 (—*N*—C$\mathbf{H}_2$—O—), 2.496 −2.423 (C$\mathbf{H}$=C$\mathbf{H}$—), 0.94-0.89 (C$\mathbf{H}$=C$\mathbf{H}$—C$\mathbf{H}_2$)$_4$C$\mathbf{H}_3$).

^{13}C-NMR spectra SA/BMF ($CDCl_3$) δ (ppm): 131-129 (**C**=**C**—O), 128 (**C**H=**C**H), 167 (**C**=O), 66-62 (**C**H—O), 125 ($\mathbf{C}_{benzene}$), 131 (carbons of s-triazine ring of melamine). The presence of these peaks confirmed the curing of SA with BMF.

Synthesis of PANI-PDMS adduct

Silane (2 g) dissolved in EMK was mechanically stirred in a reaction flask fitted with magnetic stirrer and thermometer for 5–6 h on an oil bath at 200°C. Zinc chloride (1 mg, catalyst) and ammonium persulphate (2 mg) were then added to the reaction mixture under continuous stirring. The progress of the reaction was monitored by TLC and hydroxyl value to ensure the polymerization of silane. The reaction mixture was then cooled to 0–5°C and *in situ* polymerization of aniline was carried out by the addition of ammonium per sulfate (2 mg). The formation of PANI-PDMS adduct was confirmed by FTIR and is shown in Schem. 2. The structural elucidation of PANI-PDMS adduct was also done by UV-visible while the nanostructured morphology, was confirmed with the help of X-ray and TEM analysis.

^{1}H-NMR spectra of PANI-PDMS δ (ppm): 4.5 (N$\mathbf{H}$-C_6H_6), 6.42-6.39 ($C_6\mathbf{H_6}$), 11.2 (NH-$C_6\mathbf{H_6}$).

^{13}C-NMR spectra of PANI-PDMS δ (ppm): 156 (C_6H_6). The characteristics values of ^{1}H-NMR and ^{13}C-NMR corroborate with the structure as shown in Scheme. 2.

Synthesis of PANI-PDMS dispersed SA-BMF nanocomposites

The PANI-PDMS/SA-BMF composites were prepared by mixing the different amount of PANI-PDMS (0.25 wt %, 0.5 wt %, 1 wt %) in 10% SA-BMF solution in ethyl methyl ketone. The PANI-PDMS adduct was found to be homogeneously dispersed in **SA-BMF** up to 1 wt %, beyond which it was found to be highly immiscible and nondispersible resulting in phase separation. Hence loading of PANI-PDMS beyond 1 wt % was not attempted. The mixture was continuously stirred for a period of 4–5 h at room temperature to ensure the complete mixing of PANI-PDMS adduct in SA-BMF. The constituent mixture was then placed in a rotary evaporator to remove the solvent. The formation of the PANI-PDMS/SA-BMF nanocomposites was confirmed by FTIR and UV-visible spectroscopic techniques.

CHARACTERIZATION

Spectral analysis

FTIR spectra of these polymers were taken on a PerkinElmer 1750 FTIR spectrophotometer (Perkin–Elmer Instruments, Norwalk, CT) with the help of NaCl cell. UV-visible spectra were taken on Perkin–Elmer-LAMDA-ez-221 in solution form.

Thermal analysis

Thermogravimetric analysis (TGA) was performed using the SII EXSTAR 6000 analyzer (Japan) from 40 to 800°C in nitrogen atmosphere at 20°C/min flow rate.

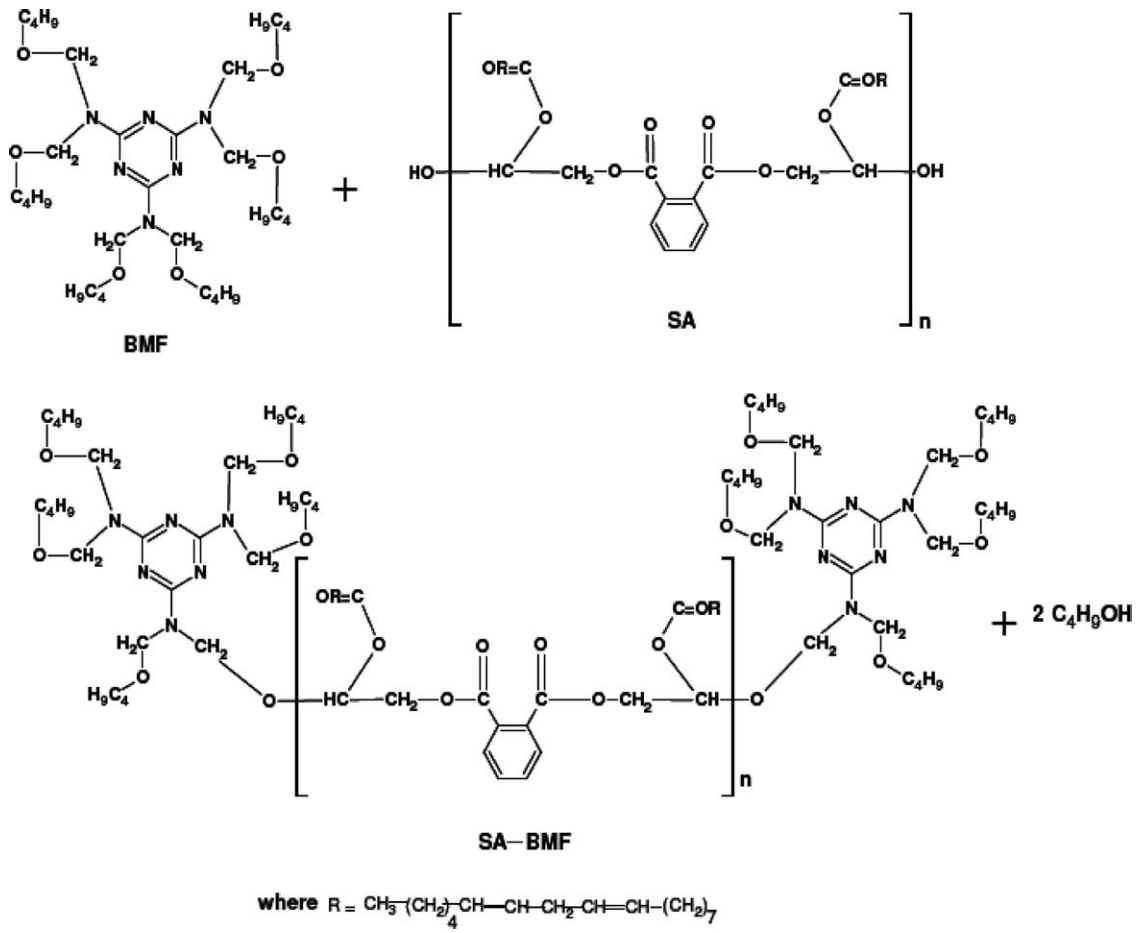

Scheme 1 Curing of SA with BMF.

Morphological analysis

X-ray diffractograms were recorded on Philips X-ray diffractometer model Philips W3710 using copper Kα radiation. Transmission electron micrographs (TEM) were taken on Morgagni 268-D TEM, FEI, USA. The samples were prepared by placing an aqueous drop of PANI-PDMS and PANI-PDMS/SA-BMF on carbon-coated copper grid, subsequently drying in air before transferring it to the microscope operated at an accelerated voltage of 120 kV.

Physicomechanical and physicochemical studies

The specific gravity (ASTM D792) and refractive index (ASTM D542) of composites were determined. The PANI-PDMS/SA-BMF nanocomposite was applied by brush on steel strips (70 mm × 30 mm × 1 mm) for the determination of specular gloss at 60° by gloss meter (modelRSPT-20; digital instrument Santa Barbara, CA), scratch hardness (BS 3900), and impact resistance (IS: 101 par 5/s-31988). For each composite, five samples were tested and their average values were determined using error bars representing standard deviation.

Electrical conductivity measurements

Conductivity of films was measured by standard four probe method using Keithley DMM 2001 and EG and G Princeton Applied Research potentiostat model 362 as current source. For each composite,

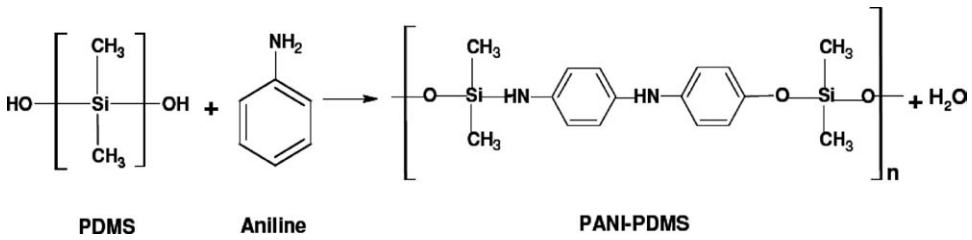

Scheme 2 Formation of PANI-PDMS adduct.

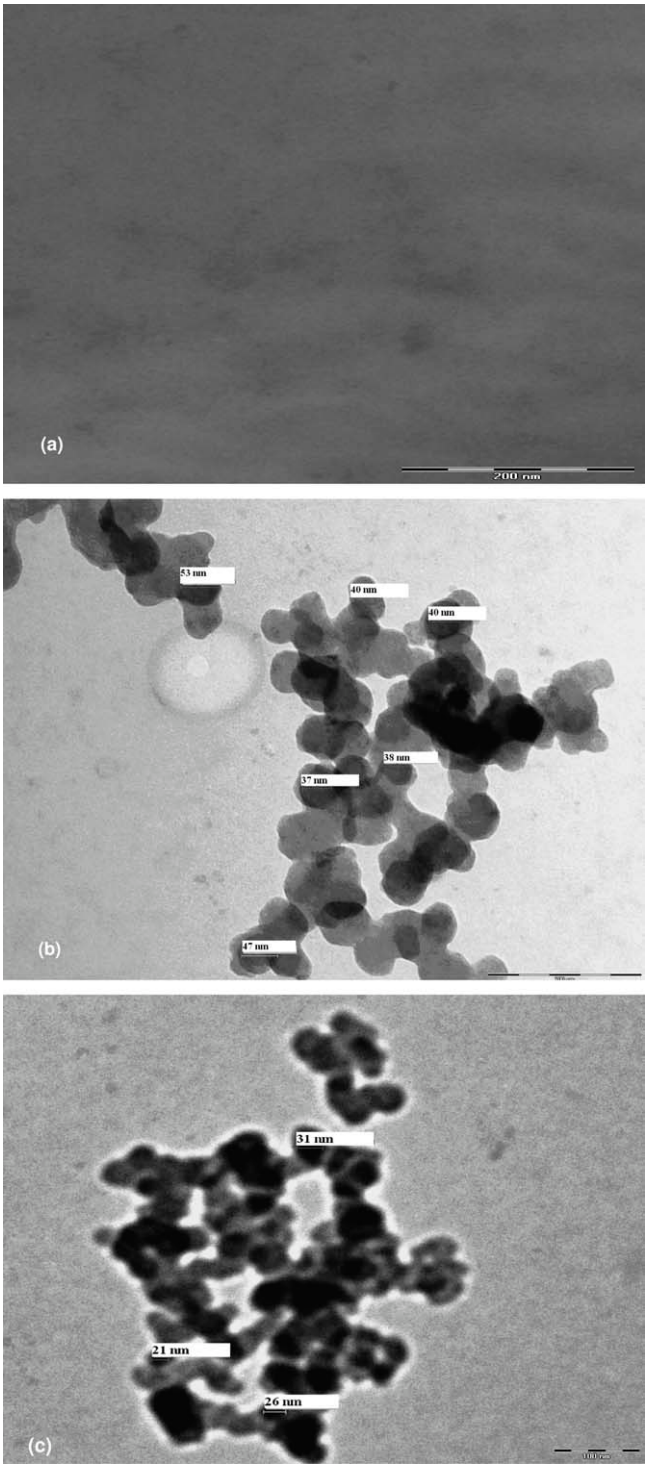

Figure 1 TEM micrographs of (a) SA-BMF (b) PANI-PDMS (c) 1-PANI-PDMS/SA-BMF.

three specimens were taken and their mean average has been reported.

RESULTS AND DISCUSSION

Morphological analysis

The microstructure of SA-BMF resin, Figure 1(a), exhibits an intimately mixed two-phase system. This can be attributed to the difference in the extent of crosslinking of BMF with SA and the molar masses of the two constituents. The dense phase corresponds to SA while the lighter regions can be correlated to BMF. The intimate mixing of SA with BMF leads to the formation of an overall homogeneous resin. The microstructure of PANI-PDMS adduct, Figure 1(b), reveals adjoining of two types of spherical nanoparticles of average size of 40 nm. The dark particles correspond to the PANI nanoparticles while the bright particles can be correlated to PDMS. The adjoining of these particles is noticed leading to the formation of a chain like structure. The TEM of 1.0-PANI-PDMS/SA-BMF, Figure 1(c), exhibits chain like dispersion of PANI-PDMS particles exhibiting an average size of 28 nm. The PANI-PDMS nanoparticles within the SA-BMF matrix appear to be globular and highly agglomerated upon increasing the loading of PANI-PDMS.

Spectral analysis

The FTIR spectrum of SA-BMF, Figure 2, revealed peaks at 3495, 2962, and 2877 cm^{-1} exhibiting OH stretching vibration present in the alkyl chain of soy oil and CH stretching vibrations respectively. The C=O stretching vibration was observed at 1724 cm^{-1} and the peaks at 1674–1500 characterized with C—C stretching of C=C aliphatic, C=C aromatic and combination band of both C=C aliphatic and C=C aromatic band The peaks at 1398, 1107, and 1100 cm^{-1} were assigned with C—O—C stretching vibration and 570 cm^{-1} with CH_2 vibration due to C—H bending of aromatic ring contributed by phthalate units. The presence of peak at 1678 cm^{-1} for CN of melamine, confirmed the incorporation of BMF in SA. The FTIR spectrum of PANI-PDMS adduct showed vibrational bands at 3415, 2694, 2314, 1708, 1419, 1165, 975, 898, 713, and 583 cm^{-1}. The

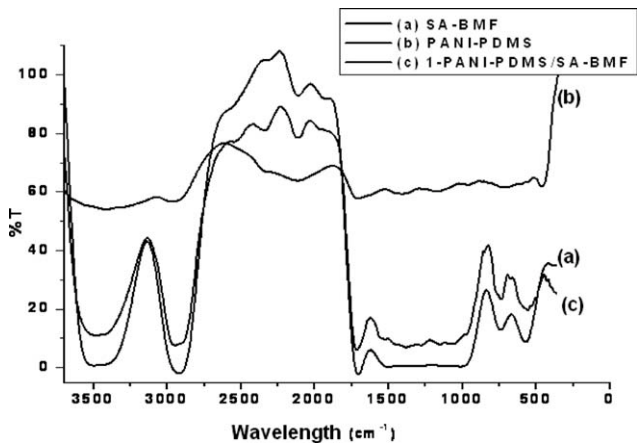

Figure 2 FTIR spectra of SA-BMF, PANI-PDMS and 1-PANI-PDMS/SA-BMF.

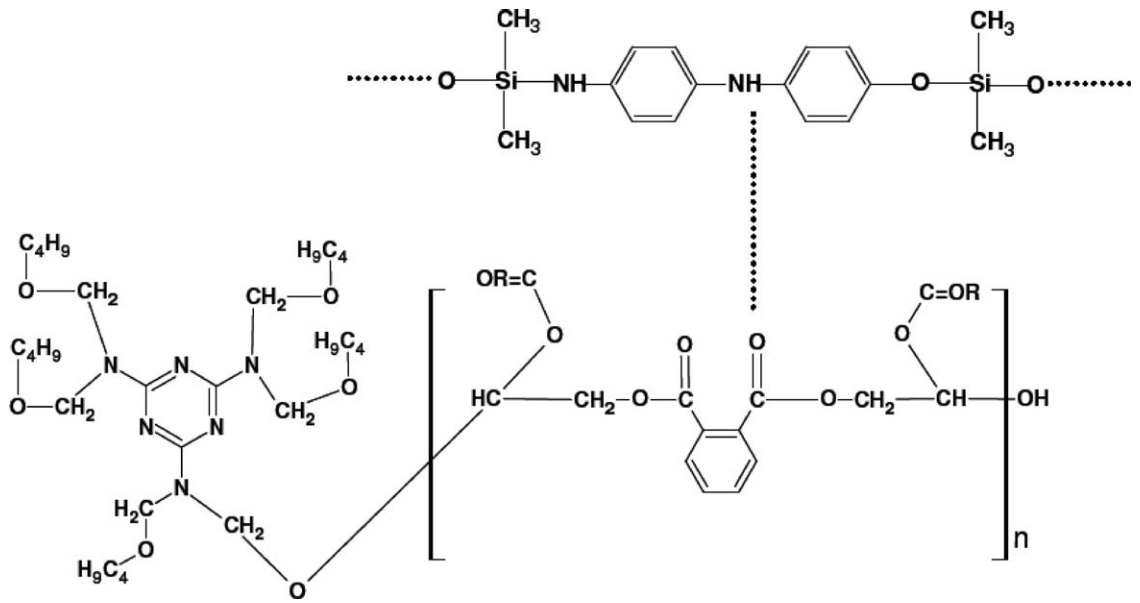

Scheme 3 Dispersion of PANI-PDMS in SA/BMF matrix.

presence of these peaks confirmed the polymerization of PDMS.[30] The broad band of —NH at 3415 cm^1 was assigned to the NH asymmetric stretching vibration of the $C_6H_4NHC_6H_4$ group correlated to the electrostatic bonding between NH of PANI and OH of PDMS. The peaks at 1708 cm^{-1} and at 1419 cm^1, 1165 cm^{-1} were attributed to the Si—N and Si—C stretching vibrations. The presence of these peaks confirmed the chemical reaction of NH of PANI with the —OH group of PDMS as shown in Scheme. 2. The FTIR spectrum of 1-PANI-PDMS/SA-BMF resin, Figure 2, reveals a shift of 15 cm^1 and 13 cm^1 in OH stretching vibration present in the alkyl chain of soy oil and C—H stretching vibrations respectively. The rest of the characteristics peaks corresponding to SA-BMF exhibited no major shift. The presence of additional peaks at 1382 cm^1 and 1537 cm^1 respectively, correspond to the C—O—C stretching vibration and C—C stretching of C=C aromatic band. As the peaks associated with SA-BMF appear to be same as incase of pristine SA-BMF, it can be concluded that 1-PANI-PDMS/SA-BMF resin exhibits a composite structure as shown in Scheme 3.

The UV-Visible spectra of PANI-PDMS adduct and PANI-PDMS/SA-BMF nanocomposites are shown in the Figure 3. The absorption peak at 350 nm can be correlated to the π-π* transition in benzene ring, which is related to the extent of conjugation of adjacent phenylene rings in the polymer chain and the charge transfer from valence band to conduction band. The absorption peak in the visible region (475, 550, 700 nm), shows the excitation of the imine units of the PANI backbone and the donor–acceptor interactions of benzenoid-quinonoid rings revealing n-π* transitions. The broad absorption peak around 650–700 nm observed in pristine PANI-PDMS can be correlated to the presence of highly delocalized electrons. The spectra of PANI-PDMS/SA-BMF composites show a blue shift of 100 nm in the polaronic transition peak which is observed at 600 nm. The increase in the intensity of the polaronic transition peaks upon higher loading of PANI-PDMS in SA-BMF and the shifting of the polaronic transition peaks confirms the restriction in the delocalization of polarons in the PANI-PDMS chains, due to electrostatic interaction via hydrogen bonding between the carbonyl group of SA-BMF and the amide of PANI-PDMS. Intense conformational changes take place in the chain configuration of PANI-PDMS upon loading in SA-BMF matrix which is noticed by the suppression of peak around 450 nm. The physical interaction of PANI-

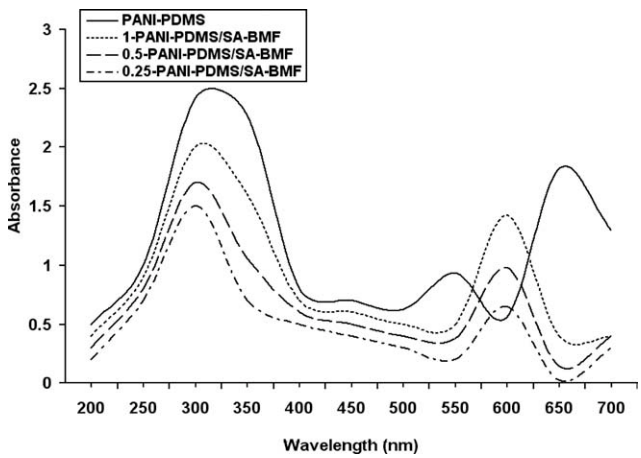

Figure 3 UV-visible spectra of PANI-PDMS and PANI-PDMS/SA-BMF nanocomposites.

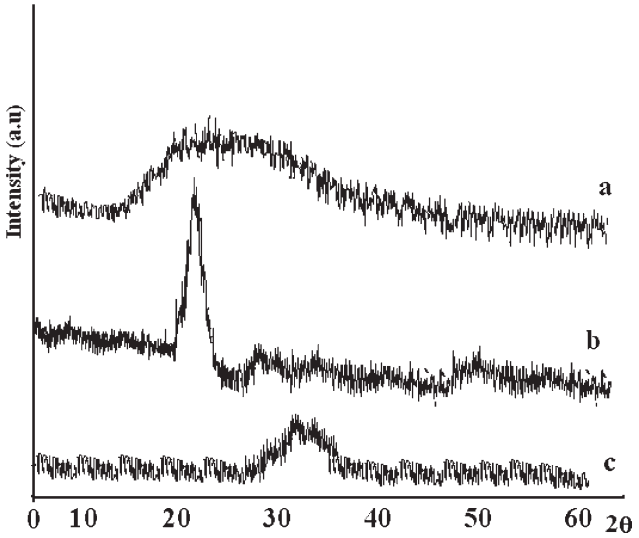

Figure 4 XRD diffractograms of (a) SA-BMF, (b) PANI-PDMS, (c) 1-PANI-PDMS/SA-BMF

PDMS chains with alkyd segments hinders the path for the charge conduction, causing a significant decrease in the conductivity of the PANI from 5.5×10^3 to 5.4×10^4 S/cm.

The value of conductivity of pristine PANI, was found to be metallic i.e., 6.0×10^3 S/cm. After the incorporation of silicon moiety in PANI, the conductivity showed a slight decrease of 0.5×10^3 S/cm. Furthermore, upon loading of 0.25 wt % of PANI-PDMS in SA-BMF, the conductivity was found to further decrease by an order and was observed to be 6.0×10^4 S/cm. As loading increased from 0.25 wt % to 1 wt %, the conductivity increased only sluggishly and was noticed to be 5.6×10^4 S/cm for 0.5-PANI-PDMS/SA-BMF and 5.4×10^4S/cm for 1-PANI-PDMS/SA-BMF. The present conductivity data do not reveal a well defined percolation threshold. Since the transition from the insulating state of the alkyd matrix to the conducting state of nanocomposites is observed at 0.5 wt % loading, it can be concluded that percolation limit falls below 1 wt %.

XRD analysis

The XRD of SA-BMF, Figure 4(a), shows a hump spanning over 20–40 Å. The presence of this broad hump indicates a predominantly amorphous structure. In case of PANI-PDMS, Figure 4(b), a pronounced peak is observed at 25 Å corresponding to a full width at half maxima (FWHM) of 3 and having an average particle size of 35 nm as calculated by Scherer equation which confirms the nanostructure of the adduct.[14] The appearance of small high angle peaks in 1-PANI-PDMS/SA-BMF nanocomposite, Figure 4(c), can be correlated to the presence of microcrystalline domains of PANI-PDMS in SA-BMF. It can be noticed that nanostructure PANI-PDMS has a significant influence on the crystallinity of alkyd matrix. The diffraction pattern in the composite shows the presence of a prominent peak around 25 Å corresponding to the presence of PANI having an average particle size of 30 nm. The peak exhibits a shift of 5 Å due to the difference in the orientation order, conformation, and electronic structure of PANI in the composite revealing microcrystalline domains. This factor is presumably responsible for the semicrystallinity of PANI-PDMS/SA-BMF nanocomposite.

TABLE I
Physico-Chemical Studies of SA-BMF and PANI-PDMS/SA-BMF Nanocomposites

Resin	Inherent viscosity (g/mL)	Specific gravity (g/cm^3)	Refractive index	Gloss (45°)
SA-BMF	0.843	1.582	1.543	85
0.25-PANI-PDMS/SA-BMF	0.9676	1.612	1.522	59
0.5-PANI-PDMS/SA-BMF	1.089	1.671	1.495	54
1.0-PANI-PDMS/SA-BMF	1.112	1.75	1.478	51

Physicochemical and physico mechanical characterization

The physicochemical properties of PANI-PDMS/SA-BMF nanocomposite are shown in Table I. The viscosity of the nanocomposites was observed to increase with the increase in the loading of the adduct which can be attributed to the restricted molecular mobility of the SA-BMF chains. The dispersion of PANI-PDMS adduct causes electrostatic interaction between OH of alkyd with NH of PANI-PDMS via hydrogen bonding as shown in Scheme. 3. The increase in the specific gravity, Table I, can be

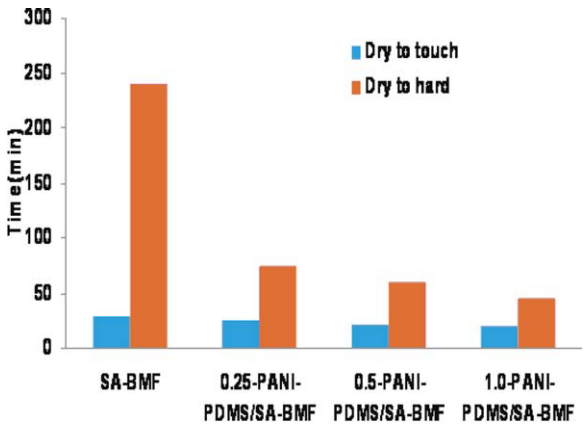

Figure 5 Dry-to-touch and Dry-to-hard times for SA-BMF and PANI-PDMS/SA-BMF nanocomposites. [Color figure can be viewed in the online issue, which is available at wileyonlinelibrary.com.]

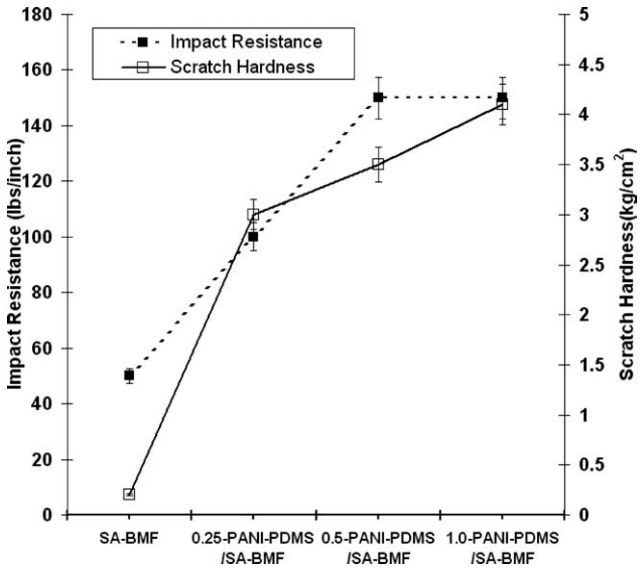

Figure 6 Correlation between scratch hardness and impact resistance.

correlated to the increase in the density of nanocomposite which confirms the dispersion of the adduct. The gloss as well as the refractive index values were found to decrease with the increase in the loading of PANI-PDMS in SA-BMF resin. This can be correlated to the dense and opaque nature of PANI-PDMS.

The dry-to-touch and dry-to-hard times of SA-BMF exhibited a remarkable decrease upon loading of PANI-PDMS adduct, Figure 5. The dry to touch time for pristine SA-BMF was found to be 30 min while the dry to hard time was found to be 240 min. The inclusion of PANI-PDMS adduct revealed a gradual decrease in dry-to-touch and dry-to-hard times which was found to be 25 and 75 min for 0.25-PANI-PDMS/SA-BMF, 22 and 60 min for 0.5-PANI-PDMS/SA-BMF, 20 and 45 min for 1-PANI-PDMS/SA-BMF nanocomposites, respectively. This can be

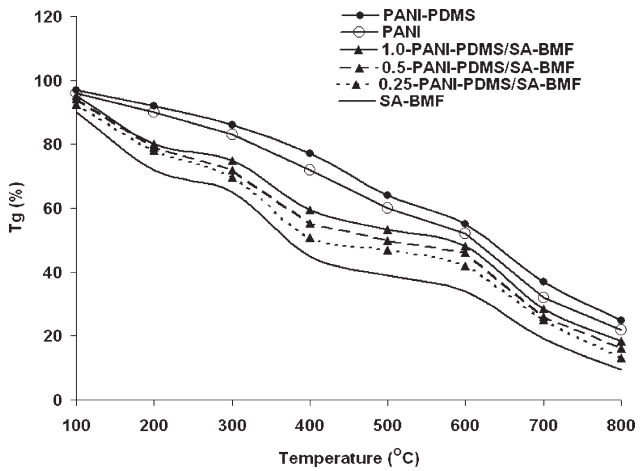

Figure 7 TGA thermograms of PANI, PANI-PDMS, SA-BMF and PANI-PDMS/SA-BMF nanocomposites

attributed to the extended crosslinked structure of the PANI-PDMS/SA-BMF nanocomposite. The correlation between scratch hardness and impact resistance, Figure 6, revealed that the scratch hardness values increased from 0.2 to 4.1 kg as the loading of PANI-PDMS in SA-BMF increased from 0.25 to 1.0 wt %. The impact resistance values also showed a gradual increasing trend with the increase in the impact from 50 to 200 kg/cm^2. This can be attributed to the intimate mixing of the two components at higher composites loadings of PANI-PDMS and the enhancement of adhesion between PANI-PDMS and SA-BMF nanocomposite with the metal surface. The presence of intense hydrogen bonding between PANI-PDMS and SA-BMF also promotes adhesion between coating and substrate.

Thermal stability

The thermal stability of the composites was compared at the temperature where 20 wt % loss occurs as the thermograms of the same show a similar decomposition pattern at this weight loss, Figure 7. In case of pristine PANI, initial thermal decomposition at 20 wt % was observed at 430°C while 50 wt % decomposition was observed at 540°C. The thermal stability of PANI-PDMS revealed 20 wt % decomposition at 440°C while 50 wt % decomposition was observed at 610°C which was quite higher than the pristine PANI. This increase in thermal stability of PANI-PDMS can be attributed to the incorporation of silicon moiety in PANI which considerably enhances the thermal stability. The initial decomposition of 20 wt % for pristine SA-BMF was found to be around 200°C, while almost 50 wt % decomposition was observed around 350°C. In case of 0.25-PANI-PDMS/SA-BMF, higher thermal stability was observed than pristine SA-BMF. The initial decomposition temperature was noticed at 350°C while around 50 wt % loss was observed at 400°C. The thermal stability of SA-BMF increased further with the increase in the loading of the PANI-PDMS and was found to be maximum for 1-PANI-PDMS/SA-BMF, exhibiting 20 wt % loss at 435°C and 50 wt % loss at 520°C, respectively. The thermal stability reveals the following trend: pristine PANI-PDMS > 1.0-PANI-PDMS/SA-BMF > 0.5-PANI-PDMS/SA-BMF > 0.25-PANI-PDMS/SA-BMF>SA-BMF. The increase in the thermal stability of the nanocomposites as compared with pristine SA-BMF at loading as low as 1 wt % of PANI-PDMS in the former presumably results due to intense hydrogen bonding between OH of alkyd and NH of PANI-PDMS as evident from the FTIR studies.

CONCLUSIONS

A nanotechnological approach was adopted to design a nanotailored PANI-PDMS reinforced SA-BMF

nanocomposite. The minimal dispersion (0.25–1 wt %) of nanostructured PANI-PDMS adduct and its intermolecular hydrogen bonding with SA-BMF matrix significantly enhances the thermal, mechanical, and morphological properties of the nanocomposites as compared with other reported system.[14] The improved properties of SA-BMF upon reinforcement with PANI-PDMS suggest its potential application as a corrosion-protective coating material. The corrosion protective studies of the PANI-PDMS/SA-BMF system are underway in our laboratory and will be published soon.

The authors wish to acknowledge the University Grants Commission (UGC) for providing the TG-DTA instrument under UGC-SAP program.

References

1. Oyama, N.; Tatsuma, T.; Sato, T.; Sotomura, T. Nature 1995, 373, 598.
2. Novak, P.; Muller, K.; Santhanam, K. S. V.; Haas, O. Chem Rev 1997, 97, 207.
3. Ryu, K. S.; Jeong, S. K.; Joo, J.; Kim, K. M. J Phys Chem B 2007, 111, 731.
4. Sengupta, P. P.; Barik, S.; Adhikari, B. Mater Manuf Process 2006, 21, 263.
5. Mansouri, J.; Burford, R. P J Memb Sci 1994, 87, 23.
6. Yin, Z. H.; Long, Y. Z.; Gu, C. Z.; Wan, M. X.; Duvail, J. L. Nanoscale Res Lett 2009, 4, 63.
7. Inzelt, G.; Pineri, M.; Schultze, J. W.; Vorotyntsev, M. A. Electrochim Acta 2000, 45, 2403.
8. Pyshkina, O. A.; Kim, B.; Korovin, A. N.; Zezin, A.; Sergeyeva, V. G.; Levon, K. Synth Met 2008, 158, 999.
9. Lippert, T.; Raimondi, F.; Wambach, J.; Wei, J.; Wokaun, A. Appl Phys A: Mater Sci Proc 1999, 69, S291.
10. Thanpitcha, T.; Sirivat, A.; Jamieson, A. M.; Rujiravanit R. J. Nanopart Res 2009, 11, 1167.
11. Bereket, G.; Hur, E.; Sahin, Y. Prog Org Coat 2005, 54, 63.
12. Ufana, R.; Ashraf, A. A.; Ashraf, S. M.; Sharif, A Prog Org Coat 2009, 65, 405.
13. Laco, J.; Villota, F. C.; Metres, F. L. Prog Org Coat 2005, 52, 151.
14. Armelin, E.; Oliver, R.; Liesa, F.; Iribarren, J. I.; Estrany, F; Aleman, C Prog Org Coat 2007, 59, 46.
15. Radhakrishnan, S.; Siju, C. R.; Mahanta, D.; Patil, S.; Madras, G. Electrochim Acta 2009, 54, 1249.
16. Yao, B.; Wang, G.; Ye, J.; Li, X. Mater Lett 2008, 62, 1775.
17. Chen, Y.; Wang, X. H.; Li, J.; Lu, J. L.; Wang, F. S. Electrochim Acta 2007, 52, 5392.
18. Jadhav, R. S.; Hundiwale, D. G.; Mahulikar, P. P. J Coat Technol Res 2009, 7, 449.
19. Oh, S.-G.; Im, S.-S. Curr Appl Phys 2002, 2, 273.
20. Menshikova, P.; Pyshkina, O. A.; Levon, K.; Sergeyev, V. G. Colloid J 2009, 71, 233.
21. Hou, S. S.; Chung, Y. P.; Chan, C. K.; Kuo, P. L. Polymer 2000, 41, 3263.
22. Ulrich, L.; Simon, W. K.; Klaus, S. R.; William, J. M. K. Macromolecules 1999, 32, 3426.
23. Alam, J.; Riaz, U.; Ashraf, S. M.; Sharif, A. J. Coat Technol Res 2008, 5, 123.
24. Alam, J.; Riaz, U.; Ahmad, S. Polym Comp 2010, 31, 32.
25. Deligoz, H.; Yalcinyuva, T.; Ozgumus, S. Eur Polym Mater 2005, 41, 771.
26. Wu, C. S.; Liu, Y. L.; Chiu, Y. S. Polymer 2002, 43, 4277.
27. Kambour, R. P. J Appl Polym Sci 1981, 26, 861.
28. Sharif, A.; Gupta, A. P.; Eram, S.; Manawwer, A.; Pandey, S. K. Prog Org Coat 2005, 54, 248.
29. Kumar, S. A.; Narayanan, T. S. N. S. Prog Org Coat 2002, 45, 323.
30. Zhou, D.; Subramaniam, S.; Mark, J. E. J Macromol Sci Part A Pure Appl Chem 2005, 42, 1.